

## **Hadamard transform photothermal deflection densitometry of electrophoretically blotted proteins**

PATRICK J. TREADO, LINDA M. BRIGGS and MICHAEL D. MORRIS\*

*Department of Chemistry, University of Michigan, Ann Arbor, MI 48109-1055 (U.S.A.)*

(First received December 12th, 1989; revised manuscript received March 22nd, 1990)

---

### ABSTRACT

Hadamard transform spatial multiplexing techniques are applied to laser densitometry in order to prevent the photo-induced degradation of sensitive materials. Photochemical and thermal degradations can often occur in point focused scanning laser densitometry. In spatial multiplexing, the excitation source is defocused and efficiently distributed throughout the sample, reducing local power density. In this paper, we describe the application of Hadamard transform spatial multiplexing to transverse photothermal deflection spectroscopy (PDS). Proteins western blotted on nitrocellulose membrane are line imaged using the Hadamard transform PDS densitometer. For comparison, the blots are imaged with a high-dynamic-range video densitometer.

---

### INTRODUCTION

Protein or western blotting<sup>1</sup> involves the transfer of electrophoretically resolved proteins to an immobilizing membrane. Proteins are transferred without loss of resolution to the surface of a nitrocellulose or other membrane and become accessible to a variety of probes including antibodies<sup>2</sup>. Immunodetection is highly specific and capable of high sensitivity (30 pg of protein). Protein blotting provides a rapid screen for detection of a gene product in a foreign host. The technique is rapid since isolation and purification of the protein does not preclude identifying it.

In addition, multiple blots can be made from a single gel if necessary for application of different detection schemes. For example, stain of total protein, or highly specific immunoassays can be performed. Also, blots have archival properties. Under certain conditions proteins blotted on nitrocellulose retain activity and can be probed as late as several months after initial immobilization. These advantages have made protein blotting an attractive technique.

Densitometry of proteins in gels is well-developed. Measurement of proteins separated by gel electrophoresis in mini-gels or separated by isoelectric focusing requires at least moderate spatial resolution (100–250  $\mu\text{m}$ ) in order to detect and

quantify closely spaced bands. Most scanning laser densitometers and video cameras can fulfill the spatial requirements. Spatial resolution in conventional laser densitometers is determined by the diameter of the focused laser beam. In video systems, spatial resolution is determined by magnification of the imaging optics. Video imaging does provide two-dimensional capability, but many inexpensive cameras lack adequate sensitivity to quantify faint bands. Laser transmission densitometers often suffer from the same problem.

A commercially available charge-coupled device (CCD) system has been employed for imaging of proteins on two-dimensional polyacrylamide gels<sup>3,4</sup>. The commercial system employs a high dynamic range, cryogenically cooled CCD camera. Despite the excellent performance, the instrument's expense limits widespread applicability for routine protein densitometry. Another two-dimensional imaging technique, electronic autofluorography, has been described<sup>5</sup>. The method detects scintillation light or fluorescence with sensitivity comparable to autoradiographic methods, but spatial resolution is poor at 400  $\mu\text{m}$ .

Photothermal lensing techniques also provide 0.5–1 ng sensitivity for gel densitometry<sup>6–9</sup>. A photothermal lens is the refractive index gradient formed by heat evolution from a light absorbing sample<sup>10,11</sup>. By probing this gradient with a laser and monitoring its positional change or its intensity after passage through the gradient, sensitive indirect absorption measurements can be made. Schlieren optics is an alternative method for measuring the refractive index gradients within protein bands. This technique has been applied to densitometry of unstained proteins as a real time monitor of protein separation in gels<sup>12</sup>. The method has poor sensitivity, 0.5  $\mu\text{g}$ , and is limited to transmissive samples only.

Conventional thermal lensing is also limited to transmissive samples, but a variant, transverse photothermal deflection spectroscopy (PDS)<sup>13</sup>, can be used for detection of samples on opaque substrates used in thin-layer chromatography (TLC)<sup>14</sup> or protein blotting.

Laser densitometry is performed with PDS by either translating the sample through the pump laser or by raster scanning the pump laser across the sample. Another indirect absorption technique, photoacoustic spectroscopy (PAS), has been applied to densitometry of proteins<sup>15</sup> on gels. This technique provides high spatial resolution, 50–100  $\mu\text{m}$ , but only moderate sensitivity with a detection limit of 0.2  $\mu\text{g}$ .

Under conditions of tight focussing for high spatial resolution and high laser power for increased sensitivity analytes can undergo photophysical or photochemical transformations. These effects can range from coagulation of colloidal stains resulting in subtle absorbance shifts to gross thermal decomposition of the stained or unstained protein.

To avoid the high laser power densities of point focused laser imaging, Hadamard spatial multiplexing has been applied to both PAS<sup>16</sup> and transverse PDS<sup>16–20</sup>. In practice, the excitation source is defocused and coded with an  $n$  element Hadamard mask before sample illumination. The power density is reduced by at least a factor of  $\sqrt{n/2}$  relative to a scanning laser densitometer at comparable spatial resolution and total laser power. In addition to a reduction in power density, these techniques allow one- and two-dimensional imaging with point detectors.

Most densitometry methods were originally developed for detection of proteins in gels. Video cameras operated in reflectance mode can be used for blots. Most other

transmission based techniques require a transparent or translucent matrix and are not easily modified for densitometry of proteins on opaque blotting substrates.

In this communication, we describe the application of Hadamard transform PDS imaging to densitometry of blotted proteins. Transverse photothermal densitometry may ultimately become the principle of a sensitive, inexpensive densitometer capable of quantifying proteins on opaque substrates. The Hadamard multiplexing allows use of higher laser power than point scanning, to maximize sensitivity or minimize measurement time.

For comparison to photothermal densitometry, we have performed video densitometry using a high dynamic range, low light level CCD camera. The CCD is cryogenically cooled and has 14 bits of dynamic range. A device of this sophistication is not typically employed for routine protein densitometry. However it should serve as a rigorous standard against which to compare the photothermal system.

More conventional and lower cost video densitometry systems employ 8-bit dynamic range cameras. With dynamic range expansion techniques, the effective range can be increased to 11 bits<sup>21</sup>. If Hadamard transform photothermal densitometry can compare favorably with the 14-bit CCD camera, then the photothermal system should have a significant performance advantage over conventional video densitometry system.

## EXPERIMENTAL

Fig. 1 is a diagram of the Hadamard transform photothermal deflection densitometer. A continuous wave Nd-YAG laser (Quantronix, Smithtown, NY, U.S.A.; Model 416), frequency doubled at 532 nm, was used to irradiate the sample. The Nd-YAG laser beam shaping optics were similar to those used previously<sup>19</sup>. A one-dimensional telescope was used to expand and roughly collimate the beam for presentation to the one-dimensional Hadamard mask. The pump beam was modulated at 13 Hz with a mechanical chopper. The spatially encoded beam was

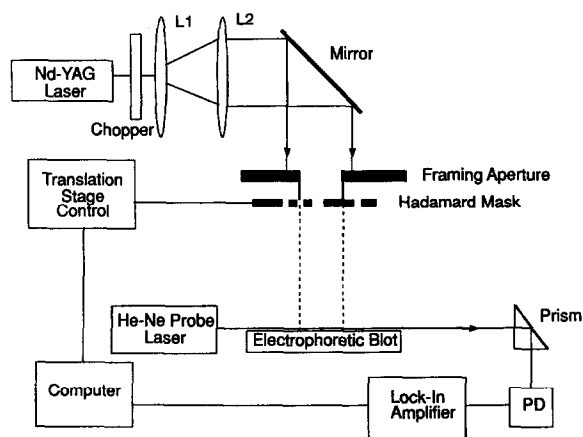


Fig. 1. Hadamard transform transverse photothermal deflection densitometer. Nd-YAG source; L1 = lens 1 (–50-mm focal length) and L2 = lens 2 (150-mm focal length): cylindrical telescope; He-Ne probe; PD: photodiode.

framed by an aperture having a width equal to the number of active resolution elements,  $n$ , times the width of a single element,  $d$ . The power delivered to the sample was approximately 20 mW. The generated refractive index gradients were probed by a He-Ne laser (Uniphase, Sunnyvale, CA, U.S.A.; Model 1101P) which was parallel to the line defined by the collimated pump beam and to the sample surface. The probe beam was detected by a position sensing photodiode. The photothermal signal was demodulated with a lock-in amplifier (Princeton Applied Research, Princeton, NJ, U.S.A.; Model 5209).

The one-dimensional Hadamard mask used in this study had 127 active elements, each element was 150  $\mu\text{m}$  wide. The mask was generated as a photographic negative on high contrast film mounted between glass plates<sup>18</sup>.

The mask was translated mechanically using a stepping motor drive (New England Affiliated Technologies, Lawrence, MA, U.S.A.; Model TM-200-SM) having 10- $\mu\text{m}$  resolution. An AT level computer (Zenith, St. Joseph, MI, U.S.A.; Model Z-248) equipped with a 12-bit analog-digital converter board (MetraByte, Taunton, MA, U.S.A.; Model DAS-16) was used for instrument control and data acquisition. The fast Hadamard transform, implemented in Turbo Pascal, was used for transformation of data from the 127-element mask.

Video densitometry was performed with a slow-scan charge-coupled device (CCD) camera (Photometrics, Tucson, AZ, U.S.A.; Series 200). The CCD is a cryogenically cooled ( $-110.0^\circ\text{C}$ ) detector suitable for low-light level imaging with 14 bits of dynamic range. Blot images were taken under tungsten illumination with a 50-mm focal length camera lens. For image processing and display the video image is transferred to a MacIntosh IIcx computer (Apple Computer, Cupertino, CA, U.S.A.) and displayed on the computer monitor using the public domain image processing program *Image* (Wayne Rasband, National Institutes of Health, Building 36, Room 2A-03, Bethesda, MD 20892, U.S.A.). For publication, the MacIntosh video monitor is photographed.

The protein samples used in this study were low-range molecular weight standards and plastocyanin, a small blue copper protein (10 500 daltons) isolated from spinach chloroplasts. The molecular weight standards are: phosphorylase B (97 400 daltons), bovine serum albumin (66 200 daltons), ovalbumin (45 000 daltons), carbonic anhydrase (31 000 daltons) and soybean trypsin inhibitor (21 500 daltons).

The proteins were separated using sodium dodecyl sulphate (SDS)-polyacrylamide gel electrophoresis<sup>22</sup> (Bio-Rad, Richmond, CA, U.S.A., Miniprotein II) in 10-17% gradient gels with 5% stacking gel. The gel thickness was 0.5 mm and sample wells were 3 mm wide. Electrophoresis was carried out at room temperature for 1 h, 30 mA constant current.

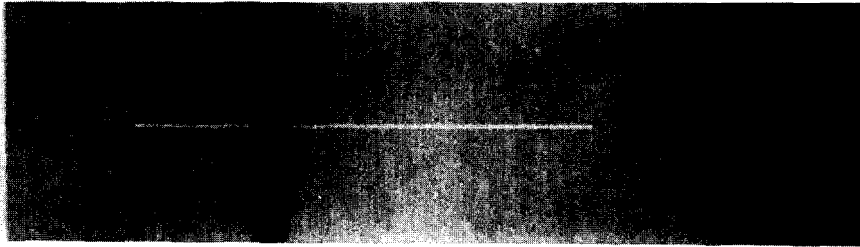
Proteins were transferred electrophoretically to a nitrocellulose substrate (Schleicher and Schuell, Keene, NH, U.S.A.) for 1 h at 240 mA. A cooling coil was employed. The molecular weight standards were stained by India ink. Plastocyanin was immunoassayed by first washing the nitrocellulose membrane in a 1:1000 dilution of antiserum for 1 h, followed by a second wash in the IgG enzyme conjugate protein A alkaline phosphatase. Polyclonal antibodies to purified spinach plastocyanin were developed by immunizing rabbits with multiple interdermal injections<sup>23</sup>.

The protein A alkaline phosphatase is visualized by Nitroblue tetrazolium chloride-5-bromo-4-chloro-3-indolyl phosphate *p*-toluidene salt (NBT-BCIP) color

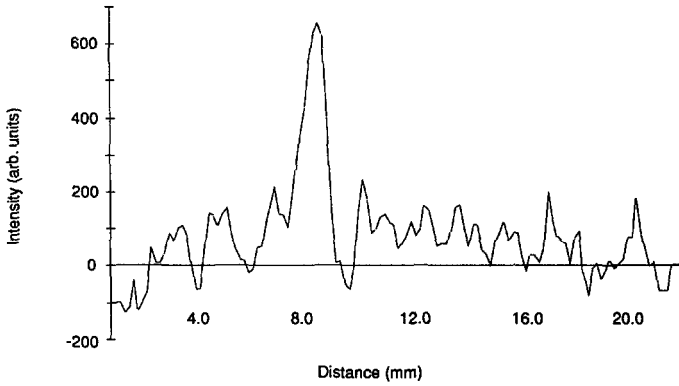
development. Characteristic purple bands were generated. The developed blots were fixed by treatment with EDTA.

RESULTS AND DISCUSSION

Fig. 2 shows images of 1  $\mu\text{g}$  of electrophoretically blotted spinach plastocyanin.



B



C

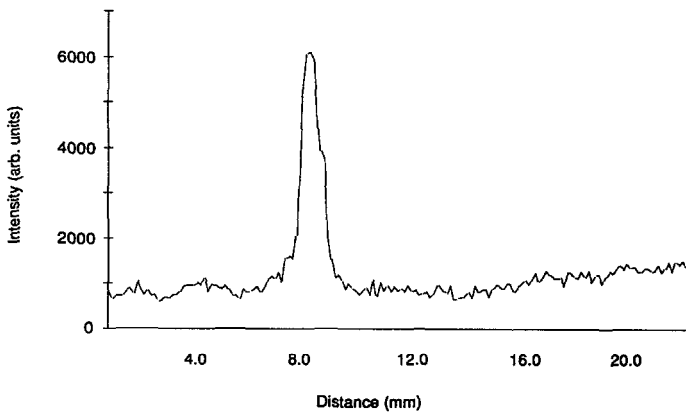


Fig. 2. Images of 5- $\mu\text{g}$  spinach plastocyanin on nitrocellulose. NBT-BCIP color development. (A) CCD camera image: white line is region where photothermal densitometry performed; (B) Photothermal electrotherogram: 1 min. acquisition; (C) Video electrotherogram: plot of video data within white line.

Fig. 2A was acquired with a slow-scan CCD camera. Fig. 2B is a Hadamard transform photothermal densitometry plot of the plastocyanin in the region defined by the white line of Fig. 2A. The one-dimensional photothermal image was acquired using the 127-element mask. The dimensions of the projected mask pattern were 2.3 cm by 0.075 cm, to yield a pixel of 0.018 by 0.075 cm. With laser power of 25 mW the power density at the sample was approximately  $0.072 \text{ W/cm}^2$ . This compares with a power density of

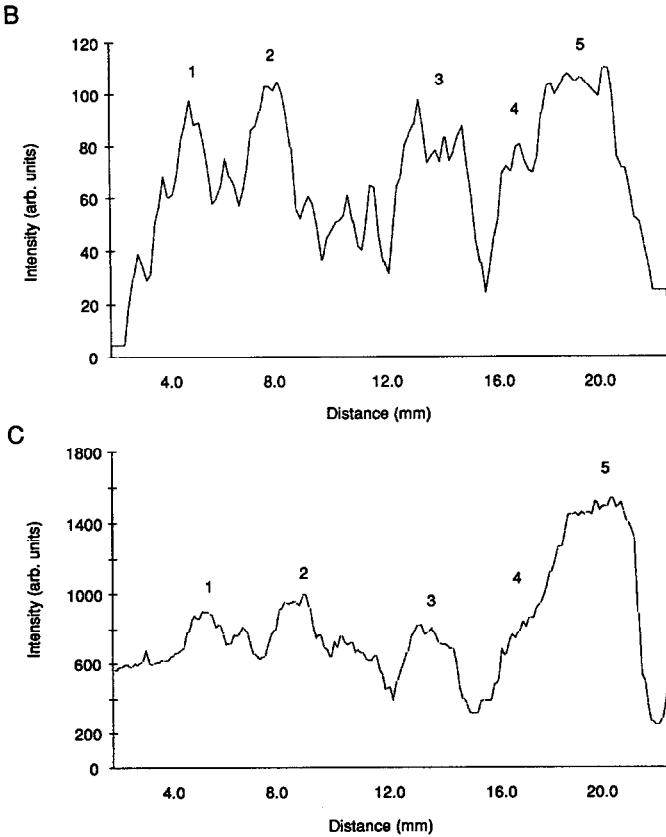
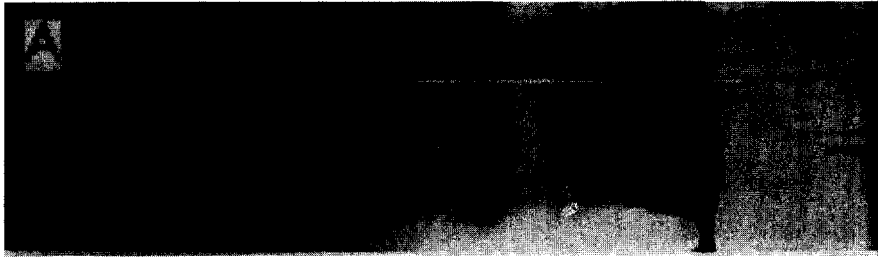


Fig. 3. Images of 5- $\mu\text{g}$  each low-range molecular weight standards. India ink stained total protein. Band 1 = phosphorylase B; 2 = bovine serum albumin; 3 = ovalbumin; 4 = carbonic anhydrase and 5 = soybean trypsin inhibitor. (A) CCD camera image: white line is region where photothermal densitometry performed; (B) photothermal electropherogram; (C) video electropherogram.

77.16 W/cm<sup>2</sup> generated by a conventional focused laser densitometer with 0.018 cm diameter spot size and 25 mW laser power. The multiplexed system reduces the power density by over three orders of magnitude. The size of the projected mask aperture at the sample, 180  $\mu$ m, indicates approximately 0.1 mrad divergence in the illumination beam. Calibration was performed using USAF 1951 standard resolution targets<sup>18</sup>. Spatial resolution of 180  $\mu$ m was enough to adequately resolve the protein bands. Protein bands were separated in general by 1 mm or more. The image was acquired using a lock-in time constant of 0.1 sec.

Fig. 2C is a densitometry plot of the same plastocyanin band. The image is a one-dimensional plot of the video data in the region where the photothermal image was taken. The band structure correlates well in both images. The photothermal image has poorer signal-to-noise ratio than the video due to several factors.

Because the probe laser is vertically positioned as close to the substrate surface as possible in order to probe the region of maximum refractive index change, photothermal deflection spectroscopy is sensitive to surface deformations in the substrate. Surface obstructions can deflect the probe beam, generating artifacts in the image. The poorer signal-to-noise ratio in fig. 2A is caused in part by sensitivity to surface deformations in the nitrocellulose substrate. These surface artifacts could be reduced by raising the probe beam relative to the substrate but at a cost to overall sensitivity. For imaging of materials on rough surfaces a trade-off between signal sensitivity and susceptibility to surface defects must be made. Storing the protein blots flat between glass plates would reduce the surface deformation artifacts.

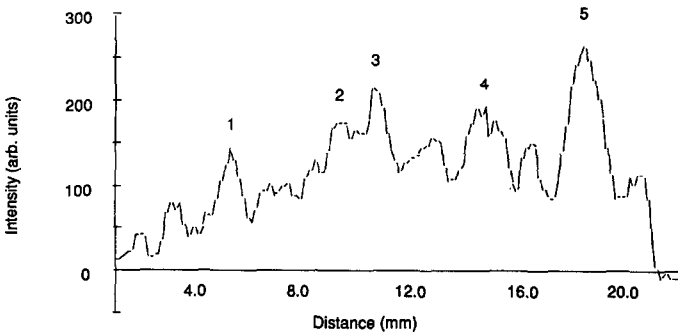
In addition to the surface deformation contribution to the photothermal background, there is a multiplex disadvantage. The multiplex disadvantage<sup>24</sup> is the redistribution throughout the data set of noise from isolated high intensity features. Random fluctuations in the probe beam due to air currents are seen as noise spikes in the raw image data. These spikes are then randomly distributed throughout the transformed data set, effectively degrading the signal-to-noise performance. Smoothing of the image reduces the background noise, but at a cost to sensitivity.

Fig. 3 shows images of 5.0  $\mu$ g quantity each of low-range molecular weight standards. Band 1 is phosphorylase B; 2: bovine serum albumin; 3: ovalbumin; 4: carbonic anhydrase; 5: soybean trypsin inhibitor. The blot was stained with India ink. Fig. 3A was obtained with the CCD video system. The electropherogram in Fig. 3B was obtained with the Hadamard transform photothermal densitometer taken in the region defined by the white line in Fig. 3A. Fig. 3C is a video electropherogram taken from the same region as the photothermal image. Carbonic anhydrase and soybean trypsin inhibitor are barely resolved in the video image but are distinct in the photothermal image.

Fig. 4 demonstrates that the sensitivity of the photothermal technique is approximately the same as video densitometry. The blot imaged in Fig. 4 has protein bands overexposed to India ink, generating a high background and smearing the protein bands. Fig. 4A is a video image of the molecular weight standards. Fig. 4B is a photothermal electropherogram of the white region of Fig. 4A. Despite the overexposure and poor separation of the proteins the photothermal technique can adequately resolve the bands. In contrast, Fig. 4C, a video electropherogram of the blot, is very poorly resolved. Note in particular the phosphorylase B band and the bovine serum albumin band which appear smeared into a single band in the video plot but are adequately imaged with the photothermal densitometer.



B



C

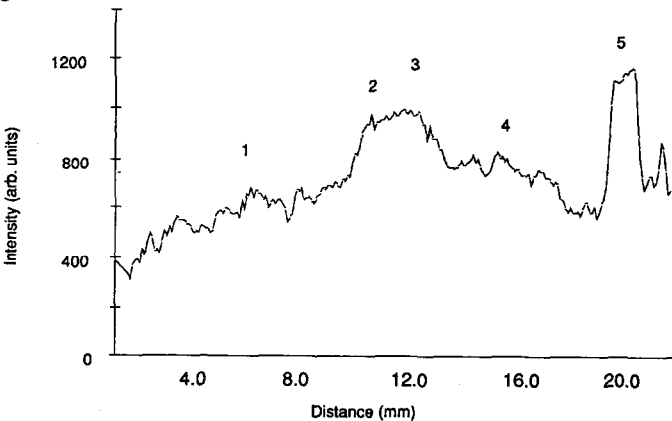


Fig. 4. Images of 5- $\mu$ g each low-range molecular weight standards. Protein overexposed to India ink. Bands: 1 = phosphorylase B; 2 = bovine serum albumin; 3 = ovalbumin; 4 = carbonic anhydrase and 5 = soybean trypsin inhibitor. (A) CCD camera image: white line is region where photothermal densitometry performed; (B) photothermal electropherogram; (C) video electropherogram.

Densitometry techniques, in general, give a direct measure of the stain associated with a particular protein, not of the protein itself. Because different proteins will take up a particular stain to varying degrees quantitative measurements are difficult. Fig. 3 and 4 demonstrate this problem. An amount of 5  $\mu$ g of each molecular weight standard has been separated, yet the peak areas are not identical for the individual proteins. In order to make quantitative measurements, experimental parameters must be controlled carefully and comparisons must be made between individual protein systems.



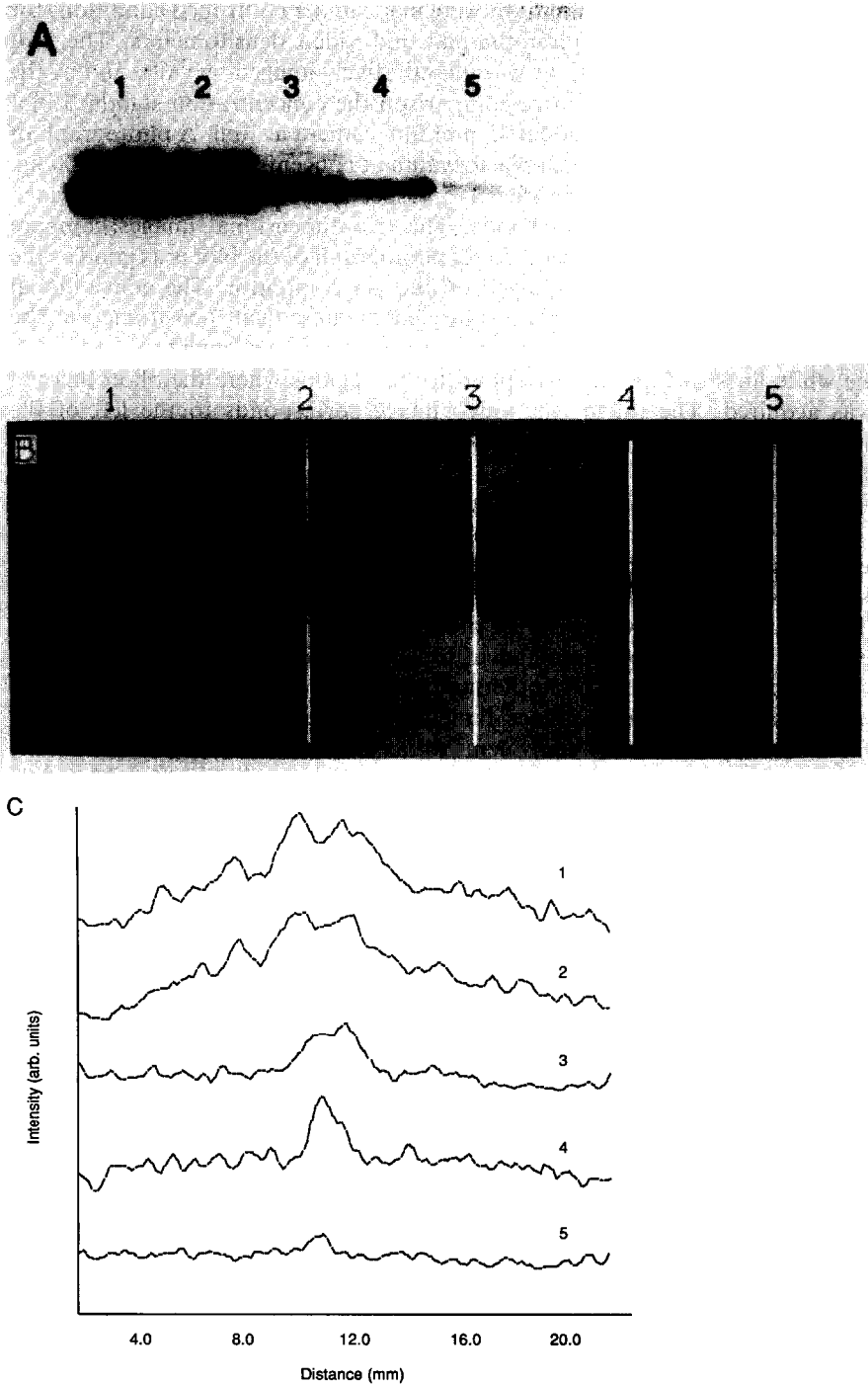


Fig. 5. Spinach plastocyanin concentration study blot. Lane 1 =  $1 \mu\text{g}$ ; 2 = 500 ng; 3 = 100 ng; 4 = 50 ng and 5 = 10 ng. NBT-BCIP color development. (A) 35-mm camera photograph of blot; (B) CCD camera image: white lines are regions where photothermal densitometry performed, top of video image corresponds to left of electrotherograms; (C) photothermal electrotherograms.

Quantitative protein determinations were made under controlled conditions for spinach plastocyanin using the photothermal and video densitometers. The blot containing the varying concentrations was quantitatively imaged by video and by the photothermal method. For qualitative comparison the concentration standard blot was photographed with a conventional 35-mm film camera as well. A photograph of the blot is shown in Fig. 5A. Spinach plastocyanin at concentrations of 1  $\mu\text{g}$ , 500 ng, 100 ng, 50 ng and 10 ng are shown in lanes 1–5, respectively. Fig. 5B is the CCD video image of the spinach plastocyanin bands. The two-dimensional images compare favorably. For presentation purposes a direct photograph of the blot is as good as the photograph of the CCD image displayed on the video monitor. The conventional photograph is purely qualitative unless subjected to subsequent densitometry. The CCD image is already available for digital analysis and enhancement.

The white lines of Fig. 5B correspond to the regions where the photothermal image was acquired. The top of the video image corresponds to the left of the photothermal plots. Fig. 5C shows the photothermal electropherograms of the same bands as in 5A and 5B.

Fig. 6 is a plot of the normalized concentration response of both densitometry systems. The upper curve, a plot of the photothermal response, is a plot of integrated peak area *versus* plastocyanin concentration. The video response, shown in the lower curve, is a plot of integrated band area *versus* plastocyanin. Both calibration curves exhibit linear response below 100 ng of protein. The photothermal response is in agreement with previous photothermal densitometry studies<sup>8</sup>. The sensitivity of both systems is comparable, but the photothermal system has approximately a factor of two worse signal-to-noise performance than the CCD camera. The photothermal densitometer is approximately equivalent to a 13-bit video camera. With the immunochemical protocol used here the plastocyanin detection limit is approximately

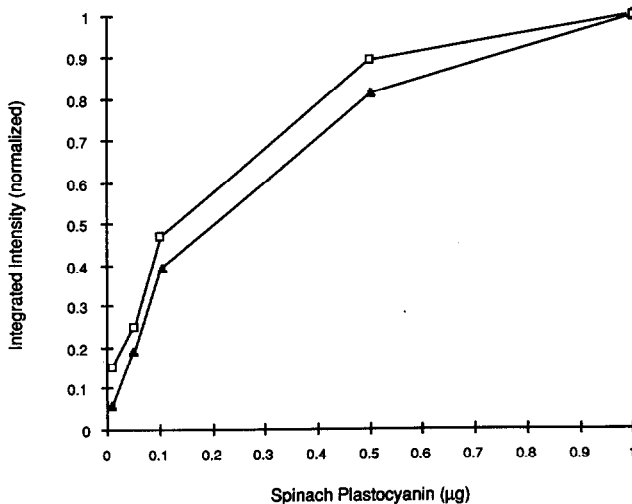


Fig. 6. Concentration response of photothermal and video densitometers.  $\blacktriangle$  = Video densitometer and  $\square$  = Hadamard transform PDS. Photothermal curve: a plot of integrated peak intensity *vs.* spinach plastocyanin concentration. Video curve: a plot of integrated band intensity *vs.* plastocyanin.

5 ng with the photothermal system and approximately 3 ng with the high dynamic range video camera. Lower detection limits can be obtained by longer color development, but only at the expense of linear dynamic range.

Video based techniques are in general faster than photothermal densitometry. Video systems comprised of a camera and 8-bit frame grabber can acquire an image at several frames a second. High-speed image acquisition allows the possibility of signal averaging for enhanced signal-to-noise performance.

Currently our photothermal system is limited to imaging one lane a minute. Our image acquisition time could be reduced significantly with modifications to the instrument. Presently, acquisition time is limited by the lock-in time constant, 0.1 s. Reducing noise in the system would reduce the time constant and subsequently the acquisition time.

Two significant noise sources are present in our system. The first is the presence of air currents which cause random fluctuations in the probe beam position. By more effectively shielding the entire experiment from the lab environment, air currents can be minimized. A second source of noise comes from the He-Ne probe laser pointing and amplitude instability. Diode lasers should provide more stable performance. With a quieter system the lock-in time constants could be reduced to 0.03 s. Image acquisition time of 20 s per lane should be readily achievable.

## CONCLUSION

Hadamard transform photothermal densitometry provides line images of photosensitive materials at high sensitivity using a point detector. It is more sensitive than conventional video densitometry using 8-, 10- or 12-bit cameras. Only the most sensitive cryogenically-cooled slow-scan CCD cameras can provide better sensitivity, but at greater cost and complexity. Although we have used laser excitation, transverse photothermal deflection signals can be excited with incoherent sources as well. A low-cost arc lamp and broad band filter could be used for sample illumination in our system. With stained proteins, monochromaticity is not essential. Another useful extension of this technique would be to employ multichannel detection to allow image acquisition across an extended region of the protein band. Multichannel detection would allow spatial averaging to reduce effects of local fluctuations in the blot surface or band structure without increasing measurement time.

## ACKNOWLEDGEMENTS

This work was supported in part by DOE Grant DE-FG02-89ER13996, in part by PHS Grant GM37006 and in part by an ACS Analytical Division Fellowship sponsored by Dow Chemical to P.J.T. L.M.B. thanks Professor V. Pecoraro for research assistantship support through NSF grant No. 022829.

## REFERENCES

- 1 H. Towbin, *Proc. Natl. Acad. Sci. U.S.A.*, 76 (1979) 4350-4354.
- 2 A. T. Andrews, *Electrophoresis*, Clarendon Press, Oxford, 1986.
- 3 C. D. Mackay, in M. J. Dunn (Editor), *Electrophoresis '86*, VCH, Weinheim, 1986, 720-722.
- 4 P. Jackson, V. E. Urwing and C. D. Mackay, *Electrophoresis*, 9 (1988) 330-339.

- 5 J. B. Davidson, in V. Neuhoff (Editor), *Electrophoresis '84*, VCH, Weinheim, 1984, 235–252.
- 6 K. Peck and M. D. Morris, *Anal. Chem.*, 58 (1986) 2876–2879.
- 7 K. Peck and M. D. Morris, *Anal. Chem.*, 58 (1986) 506–507.
- 8 K. Peck, T. Demana and M. D. Morris, *Appl. Theor. Electrophor.*, 1 (1989) 41–41–45
- 9 B. J. Jager, R. J. G. Carr and C. R. Goward, *J. Chromatogr.*, 472 (1989) 331–335.
- 10 J. P. Gordon, R. C. C. Leite, R. S. Moore, S. P. S. Porto and J. R. Whinnery, *J. Appl. Phys.*, 36 (1965) 3–6.
- 11 J. A. Sell (Editor), *Photothermal Investigations of Solids and Fluids*, Academic Press, New York, 1989.
- 12 T. Takagi, P. F. Rao and Y. Sato, in C. Schafer-Nielsen (Editor), *Electrophoresis '88*, VCH, Weinheim, 1988, 344–354.
- 13 M. D. Morris and K. Peck, *Anal. Chem.*, 58 (1986) 811A–822A.
- 14 T. I. Chen and M. D. Morris, *Anal. Chem.*, 56 (1984) 19–21.
- 15 H. Köst, U. Möller, S. Schneider and H. Coufal, in H. Harai (Editor), *Electrophoresis '83*, Walter de Gruyter, Berlin, 1984, 495–502.
- 16 H. Coufal, U. Moller and S. Schneider, *Appl. Opt.*, 21 (1982a) 116–120.
- 17 F. Fotiou and M. D. Morris, *Appl. Spectrosc.*, 40 (1986) 704–706.
- 18 F. Fotiou and M. D. Morris, *Anal. Chem.*, 59 (1987) 185–187.
- 19 F. Fotiou and M. D. Morris, *Anal. Chem.*, 59 (1987) 1446–1452.
- 20 P. J. Treado and M. D. Morris, *Appl. Spectrosc.*, 42 (1988) 1487–1493.
- 21 S. Inoué, *Video Microscopy*, Plenum Press, New York, 1986.
- 22 U. K. Laemmli, *Nature (London)*, 227 (1970) 680–685.
- 23 J. L. Vaitukaitis, *Methods Enzymol.*, 73 (1981) 46–52.
- 24 T. Hirschfeld, *Appl. Spectrosc.*, 30 (1976) 234–236.